KINETICS OF PLASMACHEMICAL PROCESSES IN BARRIER DISCHARGE ON AMBIENT AIR

I.A. Soloshenko, V.V. Tsiolko, S.S. Pogulay, A.G. Kalyuzhnaya, V.Yu. Bazhenov, A.I. Shchedrin

Institute of Physics of National Academy of Sciences of Ukraine, Kiev, Ukraine

E-mail: poguly@iop.kiev.ua

In the present paper the results of theoretical and experimental studies of kinetics of plasmachemical processes in a volume barrier discharge on ambient air are given. Calculations and experimental measurements of the concentrations of species are performed for both the discharge gap and the large volume chamber which contained reaction products pushed out of the discharge. In most cases results of the calculations are in a good agreement with the experimental data.

PACS: 52.80.Tn

1. INTRODUCTION

In the last decade an interest to the discharges at atmospheric pressure (first of all to those of barrier type) grew up considerably. First of all, it is due to attractiveness of their use for different industrial applications such as purification of exhaust gases, modification of properties of polymer surfaces, decontamination of articles from chemical and biological substances, etc. [1-4]. Studies of kinetic processes in the barrier discharge plasma on ambient air are worth of special attention because, particularly, exhaust gases are composed mainly of N_2, O_2, H_2O with admixtures of N_xO_y, CO_x and soot particles [5].

Purpose of the present work consists in researches of air humidity influence on kinetics of plasmachemical processes both in the volume barrier discharge and in remote chamber which contains reaction products pushed out of the discharge.

2. EXPERIMENTAL SETUP AND METHODS OF MEASUREMENTS

Experimental investigations were performed at two setups. The first one represented the chamber made of polymethylmethacrtylate with 80 liters volume (430x430x430 mm) and 16 discharge cells evenly placed on top wall of the chamber. Ambient air was supplied to the discharge cells through wetting/desiccation system which enabled relative humidity (RH) variations in 20…90% range at temperature of 20…22°C. Volume rate υ of the flow through each of the discharges was varied from 1 cc/s to 8 cc/s which corresponded to average residence time of the particles in the discharge gap $\tau = 2.4…0.3$ s. Particles formed in the discharge cells came to the chamber via holes having 20 mm length and 10 mm diameter, and after that passed to deactivation system via the hole of 20 mm diameter located at bottom wall of the chamber. For accomplishing optical measurements of concentrations of the species, the windows made of KU-1 quartz were placed at side walls of the chamber at distances of 65, 215 and 365 mm measured in vertical direction from top wall of the chamber.

For performing the measurements of component content of the particles immediately in the discharge volume, the second setup composed of four sequentially connected discharge cells identical to those used in the first setup was constructed. Quartz tube having 368 mm length, 26.5 mm external diameter and 1.5 mm wall thickness was used as dielectric barrier. Length of each of four discharge units was 50 mm, and the distance to central metal electrode was 1.25 mm.

Electric power for the discharge operation was supplied from the source providing maximum voltage amplitude of about 15 kV at 400 Hz frequency. Specific power introduced into the discharge was 1.5 W/cc.

For measurements of component content of the particles inside the chamber, as well as in the discharge gap, the absorption spectrometry method was implemented on a base of software-hardware complex with the use of 0.6 m MDR-23 monochromator. The experimental devices and methods of the measurements are described in more details in [6].

3. DISCHARGE MODEL

Usually [7] when determining concentrations of particles in the filamentary barrier discharge, plasma kinetics in separate current channels of the microdischarges is calculated at first, and after that in time of an order of diffusion one (~ 10^{-3} s) averaging of concentration of all components over the entire discharge volume is performed. With such approach there exists a set of parameters that are poorly known and essentially depend on design of the discharge cell and kind of gas, such as rates of occurrence of current channels, their dimensions and surface density at the discharge electrodes. Those parameters are commonly fitting ones.

Calculation presented in the present paper is based on another approach, in which power introduced into the discharge is immediately averaged over the discharge volume. With such approach, correct description is provided for processes with linear dependence on electron density, as well as for nonlinear ones with typical time of reaction being longer than the diffusion time ($t > 10^{-3}$ s). Since typical duration of chemical reactions between dissociation products in current channels does not exceed 10^{-2} s, approach used by us is valid. Besides, an advantage of this approach consists in the absence of fitting parameters.

In conducting the calculations, processes at barrier discharge electrodes and working chamber walls were not taken into account.

In calculations of the component content and concentrations of molecules and radicals formed in barrier discharge volume the following kinetic equations were used:

$$\frac{dN_i}{dt} = S_{ei} + \sum_j k_j N_j + \sum_{j,l} k_{jl} N_j N_l + \dots . \qquad (1)$$

Here N_i are concentrations of molecules and radicals; k_j, k_{jl} are rate constants of molecular processes; S_{ei} is rate of formation of products of electron-molecular reactions calculated by equation:

$$S_{ei} = \frac{W}{V}\frac{1}{\varepsilon_{ei}}\frac{W_{ei}}{\sum_j W_{ej} + \sum_j W_j} .$$

W is power introduced to barrier discharge; V is barrier discharge volume. W_{ej} is specific power spent for electron-molecular process of non-elastic scattering with threshold energy ε_{ei}:

$$W_{ei} = \sqrt{\frac{2q}{m}} n_e N_i \varepsilon_{ei} \int_0^\infty \varepsilon Q_{ei}(\varepsilon) f(\varepsilon) d\varepsilon ,$$

where $q = 1.602 \cdot 10^{-12}$ Erg/eV; m and n_e are electron mass and concentration; Q_{ei} is cross section of respective non-elastic process; $f(\varepsilon)$ is electron distribution function. W_i is specific power spent for gas heating:

$$W_i = \frac{2m}{M_i}\sqrt{\frac{2q}{m}} n_e N_i \int_0^\infty \varepsilon^2 Q_i(\varepsilon) f(\varepsilon) d\varepsilon ,$$

where M_i is mass of respective kind of molecules, Q_i is transport cross section of scattering.

Electron distribution function (EDF) was calculated from Boltzman equation in two-term approximation [6].

In calculations of the component content it was assumed that gas mixture is permanently present inside the discharge gap during the discharge glowing.

In calculation of the component content in working chamber it was assumed that the whole mixture (excluding charged particles) produced in barrier discharge volume came in spatially uniform way to the chamber with the following rates:

$$S_{ir} = \frac{N_{i\tau}}{\tau}\frac{V}{V_a} ,$$

where τ and V are mean residence time of particles in the discharge gap and the discharge volume, respectively, $N_{i\tau}$ are concentrations of separate components of the mixture for time point τ, V_a is working chamber volume.

Calculations of concentrations of molecules and radicals in working chamber were performed on a basis of the equations:

$$\frac{dN_i}{dt} = S_{ir} - S_{ia} + \sum_j k_j N_j + \sum_{j,l} k_{jl} N_j N_l + \dots$$

Here $S_{ia} = \frac{N_i}{\tau_a}$ is rate of removal of the plasma components from working chamber due to gas blow through, τ_a is a time of blow through the working chamber.

At solving of kinetic equations (1) the same elementary processes with participation of electrons as in the Table 1 of [6] were taken into consideration. The list of elementary processes with participation of uncharged particles taken into account in the present calculations was essentially modified as compared to that in Table 2 of [6]. Reactions R5, R21, R24, R26, R27, R35, R45, R48, R50, R55, R74, R75 and R77 were excluded since additional calculations have shown that mentioned reactions do not influence essentially on kinetics of the processes under study. Also, the rates of certain reactions were modified in accordance with recommendations of [8-10].

In calculations of the plasma component content in working chamber only the processes with participation of uncharged particles were taken into account.

4. RESULTS OF NUMERICAL MODELING

Effective value of adjusted electric field in the plasma E/N is an important parameter at performing the calculations of component content of the particles in barrier discharge because E/N defines electron energy distribution function (EDF) and, consequently, rate of formation of particles in the plasma. As it was shown in [11-13], during the microdischarge temporal evolution several phases can be distinguished – Townsend, a streamer, a cathode-layer formation and decay phases. The main part of radicals and excited species is created during the last phase. This effect is due to the facts that: 1) the main part of energy dissipation in the microdischarge occurs during the decay phase; 2) during this phase the main part of energy in the microdischarge is due to the electrons. Calculation [11,12] and experiment [14] also have shown, that during the decay phase E/N in the microdischarge on air does not exceed ≈ 80 Td (20 kV/cm) and decreases with time.

Thus, in the experiment adjusted electric field in the plasma changes with time whereas in our calculations it is assumed to be unchanged during the discharge glowing. As it is known, variation of electric field in the plasma influences on the EDF and, respectively, on the rates of elementary processes with participation of electrons. Thus, for correct comparison of calculations with the experiment, one should determine adjusted value E/N in the discharge plasma. For that purpose, EDF calculation was initially performed for the discharge plasma on air with relative humidity RH = 20 and 80% at different electric field values. In the EDF calculations, not only processes listed in Table 1 [6] were considered, but as well the processes of excitation of vibration levels of water molecules. Results of the calculations have shown that EDF remains practically unchanged at relative humidity growth from 20 to 80%, both with and without taking into account H_2O vibration levels. Fig.1 exhibits dependencies of normalized to unity calculated EDF for different values of electric field in the plasma at air humidity RH = 20%.

One can see from Fig.1 that: 1) EDF shape is mainly determined by the processes of interaction of electrons with N_2 molecules (particularly, EDF bend in energy range of 2…4 eV is due to excitation of vibration levels of nitrogen molecules); 2) increase of electric field value results in the increase of quantity of fast electrons. For determining electric field influence on kinetics of the processes in the discharge plasma, calculation of the

dependence of concentration of the particles on residence time was performed for different electric field values E (air relative humidity was 20 and 80%, and gas medium temperature was T_d = 425 K).

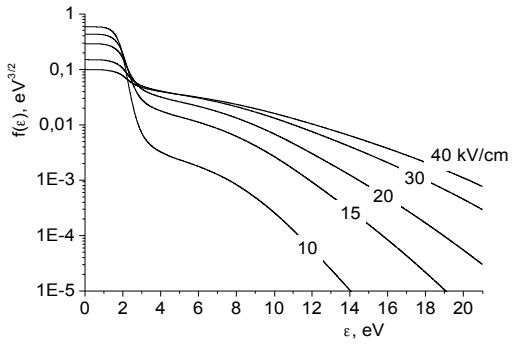

Fig.1. Dependence of calculated EDF on electric field value in discharge plasma. W_d = 1.5 W/cc, RH = 20%

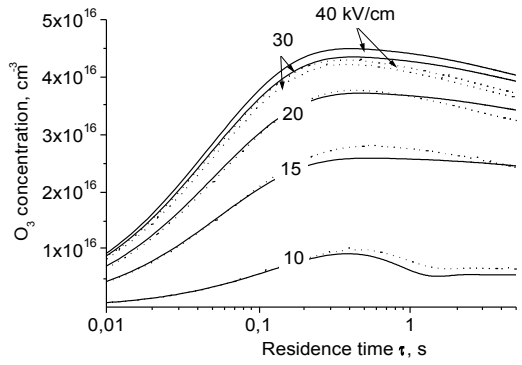

Fig.2. Calculated dependencies of O_3 concentration in the discharge gap on residence time τ at different electric field values in the plasma. W_d = 1.5 W/cc, T_d = 425 K. (Solid lines – RH = 20%, dot lines – RH = 80%)

Results of the calculations for O_3, HNO_3, HNO_2, H_2O_2 and OH species are presented in Figs.2-6. One can see from Fig.2 that for all electric field values ozone concentration at first grows up with time τ, and then starts its decrease at $\tau \approx 0.3\ldots0.4$ s. Air humidity variation practically has no influence on O_3 concentration value. One can also see from the Figure that at all τ values electric field enhancement leads to growth of ozone concentration. However, whereas E increase from 10 kV/cm to 20 kV/cm causes ozone concentration growth by several times (at $\tau \approx 0.3$ s by factor of about 7), the subsequent E increase up to 40 kV/cm results in O_3 concentration growth just by several tens percent.

Fig.3 shows calculated dependencies of concentrations of HNO_3 and HNO_2 acids on residence time τ at different electric field values in the discharge. One can see that the behavior of these dependencies with respect to both time τ and humidity is cardinally different from those in case of ozone. Particularly, nitric acid concentration (Fig.3,a) grows up monotonously with the increase of gas mixture residence time in the discharge for all values of electric field and air humidity. Besides, for all E values increase of relative humidity from 20 to 80% results in significant growth of HNO_3 concentration (for E = 20 kV/cm the concentration increases by a factor of about 3 in the range of τ variation 0.01…5 s).

However, behavior of nitric acid concentration dependence on electric field exhibits the same tendency as in case of ozone.

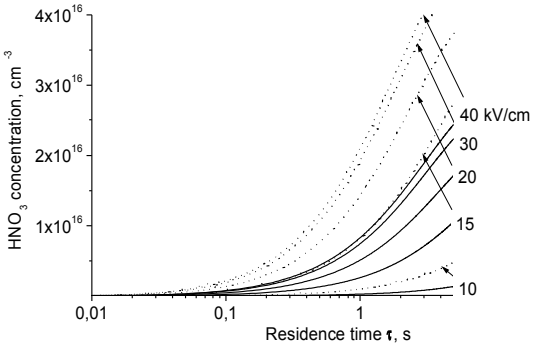

a

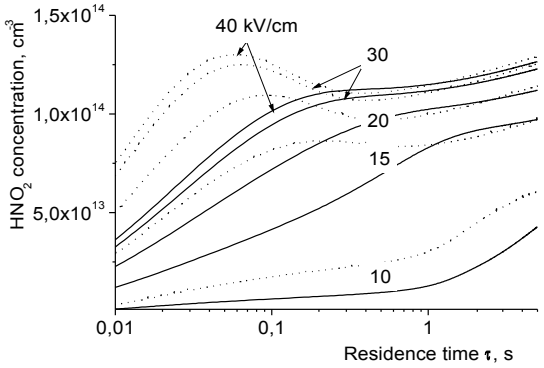

b

Fig.3. Calculated dependencies of HNO_3 (a) and HNO_2 (b) concentrations in the discharge gap on residence time τ at different electric field values in the plasma. W_d = 1.5 W/cc, T_d = 425 K. (Solid lines – RH = 20%, dot lines – RH = 80%)

At all values of air humidity HNO_3 concentration demonstrates abrupt growth (by factor of about 20 at $\tau \approx 0.3$ s) at electric field increase from 10 kV/cm to 20 kV/cm, and then at E increase up to 40 kV/cm the concentration growth slows down to several tens percent.

Unlike the case of nitric acid, behavior of HNO_2 concentration with time differs for dry (RH = 20%) and wet (RH = 80%) air. Whereas in the case of dry air nitrous acid concentration grows up practically monotonously with τ increase in the whole range of E variation, then at the humidity increase up to RH = 80% the behavior of HNO_2 concentration dependence on τ becomes different for various E values. At E = 10 kV/cm nitrous acid concentration also grows up monotonously with τ increase, but at subsequent growth of electric field value the behavior of mentioned concentration dependence changes. At first, HNO_2 concentration dependence on time reaches a maximum at $\tau \sim 0.1$ s (at that the point of reaching the maximum

shifts towards smaller time values with E increase), after that the concentration starts to decrease reaching a minimum at $\tau \sim 0.5$ s, and in subsequent it starts to grow up slowly. One can also see from the Figure that at $\tau > 0.3\ldots0.5$ s for electric field value higher than 10 kV/cm HNO_2 concentration is practically independent on air humidity. However, in spite of these peculiarities, nitrous acid concentration for both values of air humidity shows the same behavior of the dependency on electric field strength – abrupt increase of the concentration at E variation from 10 to 20 kV/cm (by a factor of 5-10 at $\tau = 0.3$ s) and slow growth at subsequent increase of electric field value.

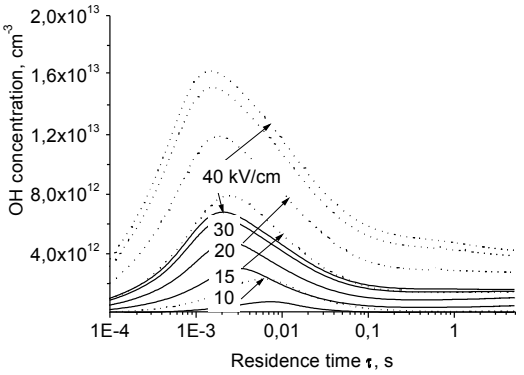

a

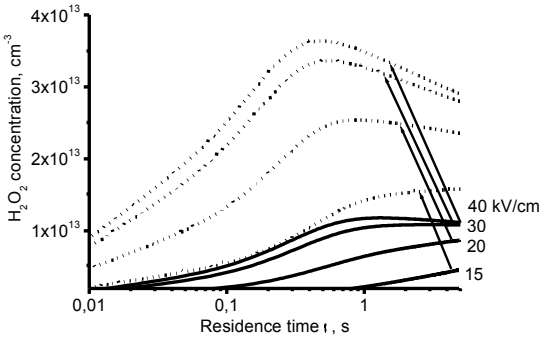

b

Fig.4. Calculated dependencies of OH (a) and H_2O_2 (b) concentrations in the discharge gap on residence time τ at different electric field values in the plasma.
W_d = 1.5 W/cc, T_d = 425K.
(Solid lines – RH = 20%, dot lines – RH = 80%)

Increase of air humidity in the discharge, first of all, should lead to the growth of OH radical concentration in result of their formation in H_2O reaction with electrons. This, in turn, leads to changes of the component concentrations, such as H_2O_2 and HO_2. Fig.4 presents calculated dependencies of OH (a) and H_2O_2 (b) concentrations in the discharge gap on residence time τ at different electric field values in the plasma.

One can see from Fig.4 that, independently on air humidity and electric field values, OH concentration reaches a maximum at $\tau \approx (2\ldots3)\cdot10^{-3}$ s and decreases at subsequent increase of residence time in the discharge.

At low air humidity hydrogen peroxide concentration grows up practically monotonously with time τ and comes to quasi-stationary value only at very strong electric field of 30…40 kV/cm. Increase of air relative humidity to 80% results in H_2O_2 concentration growth by several times (by factor of 5-6 at $\tau = 0.3$ s). Besides, at electric field values $E \geq 20$ kV/cm behavior of the dependence of concentration of hydrogen peroxide molecules on time changes - after initial growth the concentration reaches a maximum at $\tau \approx 0.3\ldots0.4$ s and after that starts its decrease.

As in cases of other considered components, OH and H_2O_2 concentrations exhibit rapid growth in 10… 20 kV/cm range of electric field variation, and essentially slower increase at subsequent growth of electric field value.

Thus, on a basis of accomplished calculations we can state that, in spite of fact that electric field increase from 10 to 40 kV/cm results in essential increase of relative quantity of fast electrons, concentrations of the species possess very weak dependence on electric field increase above ≈ 20 kV/cm for both dry and wet air. This effect is due to fact that the rate of generation of the species in the discharge depends not only on the electron energy distribution function and cross sections of elementary processes with participation of electrons, but also on the concentration of reacting species, many of which in turn depend on the rates of purely chemical reactions. At the same time, decrease of the field below ≈ 20 kV/cm causes abrupt decrease of concentrations of the particles. For that reason, use of 20 kV/cm effective electric field value in our calculations is reasonable because, on one side, excess of maximum actual electric field value in the microdischarges above 20 kV/cm gives small addition to concentration of the particles, and on another side, quantity of the particles formed during decay phase of the microdischarge (when electric field rapidly decreases below ≈ 20 kV/cm) is also small.

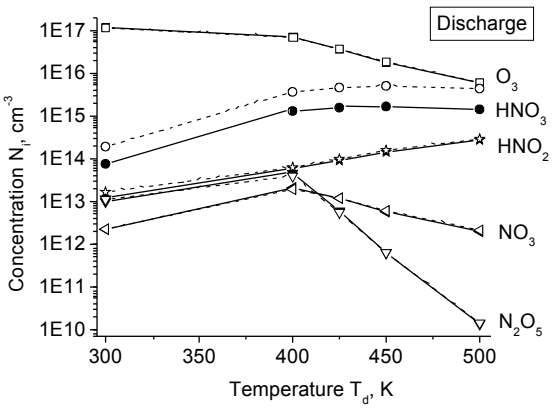

Fig.5. Calculated dependencies of the concentrations of O_3, HNO_3, HNO_2, NO_3, N_2O_5 components in the discharge gap on gas medium temperature T_d at average residence time of the particles in the discharge volume $\tau = 0.3$ s . W_d = 1.5 W/cc.
(Solid-close – RH = 20%, open-dash – RH = 80%)

In Fig.5 calculated dependencies of the concentrations of O_3, HNO_3, HNO_2, NO_3, N_2O_5 components in the discharge gap on gas medium temperature T_d at average resident time in the discharge volume $\tau = 0.3$ s are presented for different air humidity. One can see from the

Figure that at increase of air relative humidity from 20 to 80% concentrations of O_3, HNO_2, NO_3, N_2O_5 species remain practically unchanged in the whole range of T_d variation. An exclusion is represented by nitric acid HNO_3, concentration of which increases by a factor of about 3. One can see from the Figure that at $T_d \approx 425$ K concentrations of the species are: O_3 - $\approx 4 \cdot 10^{16}$ cm^{-3}; HNO_3 - $\approx 1.5 \cdot 10^{15}$ cm^{-3} (dry air), $\approx 5 \cdot 10^{15}$ cm^{-3} (wet air); HNO_2 - $\approx 1 \cdot 10^{14}$ cm^{-3}; N_2O_5 and NO_3 - $\approx 1 \cdot 10^{13}$ cm^{-3}.

In Fig.6 calculated dependencies of the concentrations of O_3, HNO_3, HNO_2, NO_3, N_2O_5 components in working chamber on gas medium temperature T_d in the discharge at average resident time $\tau = 0.3$ s are presented. (As it was already mentioned above, it was assumed in the calculations that all particles coming from the discharges to the chamber volume are instantly uniformly spread over the chamber volume and their temperature drops down to 300 K).

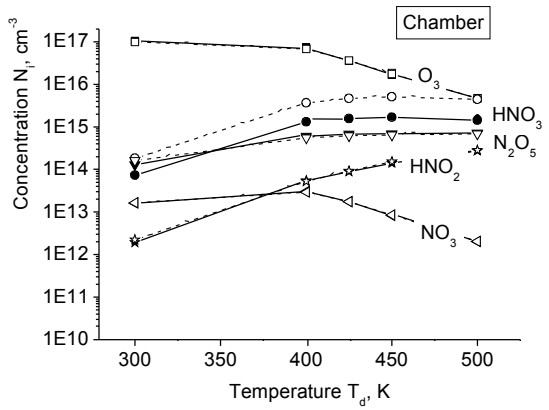

Fig.6. Calculated dependencies of the concentrations of O_3, HNO_3, HNO_2, NO_3, N_2O_5 components in working chamber on gas medium temperature in the discharge T_d at average residence time of the particles $\tau = 0.3$ s. Gas medium temperature in the chamber $T_c = 300$ K. $W_d = 1.5$ W/cc. (Solid-close – RH = 20%, open-dash – RH = 80%)

One can see from the Figure that behavior of the dependence of concentrations of the species on the temperature in the discharge gap T_d remains practically unchanged for majority of species at their transition from the discharge to the chamber. An exception is represented by N_2O_5 – whereas its concentration in the discharge decreases abruptly at $T_d \geq 400$ K, its concentration in the chamber slowly increases in the whole range of T_d growth. As well as in case of the discharge gap, increase of the humidity results only in growth of HNO_3 concentration (by a factor of about 3).

At the same temperature $T_d \approx 425$ K concentrations of the species in working chamber are: O_3 - $\approx 4 \cdot 10^{16}$ cm^{-3}; HNO_3 - $\approx 1.5 \cdot 10^{15}$ cm^{-3} (in case of dry air), $\approx 5 \cdot 10^{15}$ cm^{-3} (for wet air); HNO_2 - $\approx 1 \cdot 10^{14}$ cm^{-3}; N_2O_5 - $\approx 6 \cdot 10^{14}$ cm^{-3}, NO_3 - $\approx 1.5 \cdot 10^{13}$ cm^{-3}. Thus, we see that the concentrations of practically all species weakly change at transition from the discharge to the chamber, with an exception of only N_2O_5, concentration of which increases almost by one and half order of magnitude.

5. EXPERIMENTAL RESULTS

At accomplishing of the experiments, air relative humidity was in 22…25% range for the case of dry air, and in 80…85% range for the case of wet air. Prior to performing the measurements, the discharge setup and the chamber were blown through by air with required humidity for 40…60 minutes. Measurements of rotational temperature of nitrogen molecules T_{rot} had shown that rotational temperature was (410 ± 12) K for dry air and (430 ± 15) K for wet air. In Fig.7 the comparison between calculation results and experimental measurements of the concentrations of studied species in working chamber is presented for the cases of dry and wet air use.

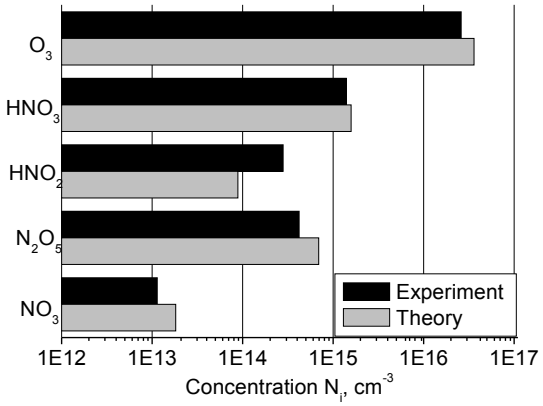

a

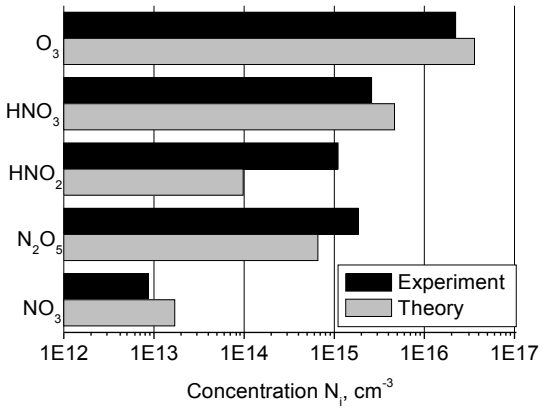

b

Fig. 7. Comparison of experimental and calculated component concentrations in working chamber for dry (a) and wet (b) air. Average residence time of the particles in the discharge volume $\tau = 0.3$ s, $T_d = 425$K, specific power in the discharge $W_d = 1.5$ W/cc. Experimental data are given for 30-th minute of accumulation of the particles in the chamber

One can see from the Figure that calculation results are in good enough agreement with experimental data. An exception is represented by the results for HNO_2 and N_2O_5 species obtained for the case of wet air use. Exper-

imentally measured HNO_2 concentration exceeds calculated value by about one order of magnitude, and N_2O_5 concentration – by a factor of about 3.

Analogous results were obtained at comparison of calculation results with experimental data for the discharge gap. As in case of the chamber, calculated and experimentally measured O_3, HNO_3 and NO_3 concentrations are in a good agreement, whereas experimentally measured HNO_2 concentration exceeds calculated one by about one order of magnitude. Possible reason for such mismatch may be due to influence of the processes at the discharge electrodes, as well as those on the chamber wall.

REFERENCES

1. U. Kogelschatz // *Plasma Chem. Plasma Process.* 2003, v.23, №1, p.1-46.
2. U. Kogelschatz // *Plasma Phys. Control. Fusion*. 2004, v.46, p.B63 – B75.
3. M. Laroussi, G.S. Sayler, B.B. Glascock, et al. // *IEEE Trans. Plasma Sci*. 1999, v.27, №1, p.34-45.
4. V.A. Khomich, I.A. Soloshenko, V.V. Tsiolko, et al. // *Proceedings of International Symposium on High Pressure, Low Temperature Plasma Chemistry (HAKONE VII), Greifswald, Germany*, September 10-13, 2000, p.26-32.
5. J.L. Huego, J.P. Espinos, A. Caballero, et al. // *Carbon*. 2007, v.45, p.89-96.
6. I.A. Soloshenko, V.V. Tsiolko, V.Yu. Bazhenov, et al. // *Plasma Sources Sci. Techn*. 2007, v.16, p.56-66.
7. I. Stefanovic, N.K. Bibinov , A.A. Deryugin, et al. // *Plasma Sources Sci. Techn.* 2001, v.10, p.406-411.
8. R. Atkinson, D.L. Baulch, R.A. Coxet, et al. // *Atmos. Chem. Phys*. 2004, v.4, p.1461-1489.
9. R. Atkinson, D.L. Baulch, R.A. Coxet, et al. // *Chem. Ref. Data.* 1989, v.18, p.881-911.
10. W.B. DeMore, S.P. Sander, D.M. Golden, et al. // *JPL Publication 97–4*. 1997, p.1-24.
11. D. Braun, V. Gibalov, G. Pietsch // *Plasma Sources Sci. Technol*. 1992, v.1, p.166-172.
12. G. Pietsch, V. Gibalov // *Pure Appl. Chem*. 1998, v.70, p.1169-1174.
13. G. Stainle, D. Neundorf, W. Hiller, and M. Pietralla // *J. Phys. D: Appl. Phys*. 1999, v.32, p.1350-1356.
14. H.E. Wagner, K.V. Kozlov, R. Brandenburg, and P. Michel // *Proceedings of International Symposium on High Pressure, Low Temperature Plasma Chemistry (HAKONE VIII), Greifswald, Germany*, 2002.

Статья поступила в редакцию 08.05.2008 г.

КИНЕТИКА ПЛАЗМОХИМИЧЕСКИХ ПРОЦЕССОВ В БАРЬЕРНОМ РАЗРЯДЕ НА АТМОСФЕРНОМ ВОЗДУХЕ

Л.А. Солошенко, В.В. Циолко, С.С. Погуляй, А.Г. Калюжная, В.Ю. Баженов, А.И. Щедрин

Приведены результаты теоретических и экспериментальных исследований кинетики плазмохимических процессов в объеме барьерного разряда на окружающем воздухе. Проведены расчеты и экспериментальные измерения концентраций компонентов как в разрядном промежутке, так и в камере большого объема, которая содержала продукты реакции разряда. В большинстве случаев результаты вычислений находятся в хорошем соответствии с экспериментальными данными.

КІНЕТИКА ПЛАЗМОХІМІЧНИХ ПРОЦЕСІВ У БАР'ЄРНОМУ РОЗРЯДІ НА АТМОСФЕРНОМУ ПОВІТРІ

Л.А. Солошенко, В.В. Циолко, С.С. Погуляй, А.Г. Калюжна, В.Ю. Баженов, А.І. Щедрін

Наведено результати теоретичних і експериментальних досліджень кінетики плазмохімічних процесів в об’ємі бар'єрного розряду на навколишнім повітрі. Проведено розрахунки і експериментальні виміри концентрацій компонентів як у розрядному проміжку, так і у камері великого об’єму, яка містила продукти реакції розряду. У більшості випадків результати обчислень перебувають у гарній відповідності з експериментальними даними.